Electronic Supplementary Information (ESI) for

A modular synthesis approach to multinuclear heterometallic oxo clusters in polyoxometalates

Takuo Minato, Kosuke Suzuki,* Yusuke Ohata, Kazuya Yamaguchi, and Noritaka Mizuno*

Department of Applied Chemistry, School of Engineering, The University of Tokyo

Materials: Acetonitrile (Kanto Chemical), acetone (Kanto Chemical), ethanol (Kanto Chemical), ethyl acetate (Kanto Chemical), 1,2-dichloroethane (Kanto Chemical), diethyl ether (Kanto Chemical), $CrCl_2$ (Aldrich), $Mn(acac)_3$ (Aldrich), $Lu(acac)_3 \cdot 2H_2O$ (Aldrich), AgOTf (Aldrich), and CH_3COONa (Kanto Chemical) were used as received. $TBA_4H_6[A\text{-}\alpha\text{-}SiW_9O_{34}] \cdot 2H_2O$ was synthesized according to the reported procedure.[S1]

Instruments: IR spectra were measured on JASCO FT/IR-4100 using KBr disks. UV-Vis spectra were measured on JASCO V-570 using 1 cm quartz cell. Cold-spray ionization (CSI) mass spectra were recorded on JEOL JMS-T100CS. Thermogravimetric and differential thermal analyses (TG-DTA) were performed on Rigaku Thermo plus TG 8120. ICP-AES analyses for Cr, Mn, Lu, Ag, Si, and W were performed with Shimadzu ICPS-8100. Elemental analyses (for C, H, and N) were performed on Elementar vario MICRO cube at the Elemental Analysis Center of School of Science of the University of Tokyo.

X-ray Crystallography: Diffraction measurements were made on a Rigaku MicroMax-007 Saturn 724 CCD detector with graphic monochromated Mo Kα radiation (λ = 0.71069 Å, 50 kV, 24 mA) at 123 K. The data were collected and processed using CrystalClear[S2] and HKL2000.[S3] Neutral scattering factors were obtained from the standard source. In the reduction of data, Lorentz and polarization corrections were made. The structural analyses were performed using CrystalStructure[S4] and WinGX.[S5] All structures were solved by SHELXS-97 (direct methods) and refined by SHELXL-2014.[S6] The metal atoms (Cr, Mn, Lu, Ag, Si, and W) and oxygen atoms in the POM frameworks were refined anisotropically, and the organic ligands, solvents of crystallization, and TBA

cations were refined isotropically. CCDC-1540839 ($\mathbf{I_{Cr}}$), -1540840 ($\mathbf{II_{CrMn4}}$), -1540841 ($\mathbf{III_{CrMn4Ag2}}$), -1540842 ($\mathbf{IV_{CrMn4Lu2}}$), and -1540843 ($\mathbf{V_{CrMn4Lu2Ag2}}$) contain the supplementary crystallographic data for this paper. The data can be obtained free of charge via www.ccdc.cam.ac.uk/conts/retrieving.html (or from the Cambridge Crystallographic Data Centre, 12, Union Road, Cambridge CB2 1EZ, UK; Fax: (+44) 1223-336-033; or deposit@ccdc.cam.ac.uk).

Bond Valence Sum (BVS) Calculations: The BVS values were calculated by the expression for the variation of the length r_{ij} of a bond between two atoms i and j in observed crystal with valence V_i.

$$V_i = \sum_j \exp\left(\frac{r_0' - r_{ij}}{B}\right)$$

where B is constant equal to 0.37 Å, r'_0 is bond valence parameter for a given atom pair.[S7]

Magnetic Susceptibilities: Magnetic susceptibilities of polycrystalline samples were measured on Quantum Design MPMS-XL7. Direct current (dc) magnetic susceptibility measurements were carried out between 1.9 and 300 K under 0.1 T magnetic field. Diamagnetic corrections were applied by the diamagnetisms of the sample holder and $TBA_4H_6[A\text{-}\alpha\text{-}SiW_9O_{34}]\cdot 2H_2O$. The magnetic interactions were analyzed by fitting the temperature-dependence of magnetic susceptibilities with the following isotropic spin Heisenberg–Dirac–van Vleck Hamiltonian where J_1 and J_2 represent exchange interactions of Cr^{3+}–Mn^{3+} and Mn^{3+}–Mn^{3+}, respectively:

$$\boldsymbol{H} = -2J_1(\boldsymbol{S}_{\mathrm{Cr}}\cdot\boldsymbol{S}_{\mathrm{Mn1}} + \boldsymbol{S}_{\mathrm{Cr}}\cdot\boldsymbol{S}_{\mathrm{Mn2}} + \boldsymbol{S}_{\mathrm{Cr}}\cdot\boldsymbol{S}_{\mathrm{Mn3}} + \boldsymbol{S}_{\mathrm{Cr}}\cdot\boldsymbol{S}_{\mathrm{Mn4}}) - 2J_2(\boldsymbol{S}_{\mathrm{Mn1}}\cdot\boldsymbol{S}_{\mathrm{Mn2}} + \boldsymbol{S}_{\mathrm{Mn3}}\cdot\boldsymbol{S}_{\mathrm{Mn4}}) \quad \text{(Eq S1)}$$

The analyses were carried out by using the PHI program.[S8] The g values for Cr^{3+} and Mn^{3+} were fixed to 2, which is typical for Cr^{3+} and Mn^{3+}.

Synthesis and Characterization of $Cr(CH_3COO)_2\cdot H_2O$: $Cr(CH_3COO)_2\cdot H_2O$ was synthesized in reference to the reported procedure[S9] by using $CrCl_2$ instead of $CrCl_3$ to omit reduction process of $CrCl_3$. An aqueous solution (6 mL) of CH_3COONa (1.74 g, 21.3 mmol) was added to an aqueous solution (1.5 mL) of $CrCl_2$ (200 mg, 1.63 mmol) under Ar atmosphere. The red precipitate formed was isolated by filtration and successively washed with water (8

mL), ethanol (5 mL), and diethyl ether (20 mL) to afford $Cr(CH_3COO)_2 \cdot H_2O$ (264.7 mg, 87% yield based on $CrCl_2$). IR (KBr pellet): 3490, 3374, 3271, 2988, 2936, 2468, 2384, 1648, 1577, 1453, 1421, 1354, 1052, 1031, 693, 682, 626, 539, 408, 383, 303, 254 cm^{-1}.

Synthesis and Characterization of $TBA_7H_{10}[(A\text{-}\alpha\text{-}SiW_9O_{34})_2Cr]\cdot H_2O\cdot 0.5C_2H_4Cl_2$ ($\mathbf{I_{Cr}}$): To a deaerated mixed solvent of acetone and water (17:3, v/v, 24 mL), $Cr(OAc)_2 \cdot H_2O$ (69.2 mg, 368 μmol) and $TBA_4H_6[A\text{-}\alpha\text{-}SiW_9O_{34}]\cdot 2H_2O$ (800 mg, 247 μmol) were added in this order, and the resulting deep blue solution was stirred for 1 h at room temperature (ca. 20°C) under Ar atmosphere. Then, deaerated ethyl acetate (500 mL) was added to the solution and blue precipitate formed was isolated by filtration. After the blue powder was dissolved in 1,2-dichloroethane (18 mL), O_2 gas was bubbled into the deep blue solution for 3 min. After diethyl ether (8.2 mL) was added, the solution was kept at 30°C. The yellowish green crystals of $\mathbf{I_{Cr}}$ suitable for X-ray crystallographic analysis were obtained after 1 day (271.4 mg, 35% yield based on $TBA_4H_6[A\text{-}\alpha\text{-}SiW_9O_{34}]\cdot 2H_2O$). IR (KBr pellet): 2962, 2936, 2874, 1634, 1485, 1382, 1152, 1107, 1060, 1016, 991, 956, 890, 811, 775, 687, 560, 534, 456, 376, 361, 255 cm^{-1}; positive ion MS (CSI, 1,2-dichloroethane): *m/z* 3331 (calcd. 3330.8) $[TBA_9H_6CrSi_2W_{18}O_{66}]^{2+}$, 6419 (calcd. 6419.0) $[TBA_8H_6CrSi_2W_{18}O_{66}]^{+}$; elemental analysis calcd (%) for $TBA_7H_{10}[(SiW_9O_{34})_2Cr]\cdot H_2O\cdot 0.5C_2H_4Cl_2$ ($C_{113}H_{266}ClN_7O_{69}Si_2CrW_{18}$), C 21.61, H 4.27, N 1.56, Si 0.89, Cr 0.83, W 52.69; found, C 21.36, H 4.25, N 1.54, Si 0.87, Cr 0.81, W 52.59.

Synthesis and Characterization of $TBA_7[(A\text{-}\alpha\text{-}SiW_9O_{34})_2CrMn_4(OH)_2]\cdot 1.5H_2O$ ($\mathbf{II_{CrMn4}}$): $Mn(acac)_3$ (9.5 mg, 27.0 μmol) was added to a 1,2-dichloroethane solution (4 mL) of $\mathbf{I_{Cr}}$ (42.9 mg, 6.8 μmol), and the resulting solution was stirred for 1 h at room temperature (ca. 20°C). Then, diethyl ether (3 mL) was added and the solution was filtered off. The green crystals of $\mathbf{II_{CrMn4}}$ suitable for X-ray crystallographic analysis were obtained after 1 day (31.8 mg, 72% yield based on $\mathbf{I_{Cr}}$). IR (KBr pellet): 3503, 2873, 2360, 2342, 1635, 1483, 1383, 1153, 1106, 1016, 957, 936, 876, 786, 711, 649, 553, 532, 410, 402, 389, 373, 333, 254 cm^{-1}; positive ion MS (CSI, 1,2-dichloroethane): *m/z* 3471 (calcd. 3470.6) $[TBA_9H_2Si_2W_{18}O_{70}CrMn_4]^{2+}$, 6699 (calcd. 6698.7)

$[TBA_8H_2Si_2W_{18}O_{70}CrMn_4]^+$; elemental analysis calcd (%) for $TBA_7[(SiW_9O_{34})_2CrMn_4(OH)_2]\cdot 1.5H_2O$ ($C_{114}H_{257}N_7O_{71.5}Si_2CrMn_4W_{18}$), C 20.75, H 4.00, N 1.51, Si 0.87, Cr 0.80, Mn 3.39, W 51.04; found, C 20.72, H 3.91, N 1.50, Si 0.82, Cr 0.70, Mn 3.18, W 48.84.

Synthesis and Characterization of $TBA_5[(A\text{-}\alpha\text{-}SiW_9O_{34})_2CrMn_4(OH)_2\{Ag(CH_3CN)\}_2]\cdot H_2O$ ($III_{CrMn4Ag2}$): To an acetonitrile solution (2 mL) of $\mathbf{II_{CrMn4}}$ (100 mg, 15.4 μmol), AgOTf (7.9 mg, 21.6 μmol) was added, and the resulting solution was stirred for 4 h at room temperature (ca. 20°C). Then, diethyl ether (3.0 mL) was added to the solution and the solution was filtered off. The green crystals of $\mathbf{III_{CrMn4Ag2}}$ suitable for X-ray crystallographic analysis were obtained after 1 day (72.5 mg, 75% yield based on $\mathbf{II_{CrMn4}}$). IR (KBr pellet): 3513, 2962, 2936, 2874, 2041, 1629, 1484, 1382, 1269, 1152, 1106, 1018, 964, 940, 925, 882, 789, 647, 536, 452, 388, 373, 332, 310, 294, 286, 282, 270, 256 cm^{-1}; positive ion MS (CSI, acetonitrile): *m/z* 3336 (calcd. 3336.0) $[TBA_7H_2Si_2W_{18}O_{70}CrMn_4Ag_2]^{2+}$, *m/z* 3403 (calcd. 3403.3) $[TBA_8H_2Si_2W_{18}O_{70}CrMn_4Ag]^{2+}$, 6430 (calcd. 6429.5) $[TBA_6H_2Si_2W_{18}O_{70}CrMn_4Ag_2]^+$, 6564 (calcd. 6564.1) $[TBA_7H_2Si_2W_{18}O_{70}CrMn_4Ag]^+$; elemental analysis calcd (%) for $TBA_5[(SiW_9O_{34})_2CrMn_4(OH)_2\{Ag(CH_3CN)\}_2]\cdot H_2O$ ($C_{84}H_{190}Ag_2CrMn_4N_7O_{71}Si_2W_{18}$), C 16.05, H 3.05, N 1.56, Si 0.89, Cr 0.83, Mn 3.50, Ag 3.43, W 52.63; found, C 16.10, H 3.00, N 1.57, Si 0.82, Cr 0.81, Mn 3.25, Ag 3.36, W 51.80.

Synthesis and Characterization of $TBA_7[(A\text{-}\alpha\text{-}SiW_9O_{34})_2CrMn_4O_2\{Lu(C_5H_7O_2)_2\}_2]\cdot 3C_2H_4Cl_2\cdot H_2O$ ($IV_{CrMn4Lu2}$): To a 1,2-dichloroethane solution (6 mL) of $\mathbf{II_{CrMn4}}$ (136.6 mg, 21.1 μmol), $Lu(acac)_3\cdot 2H_2O$ (42.8 mg, 84.4 μmol) was added, and the resulting solution was stirred for 24 h at room temperature (ca. 20°C). After diethyl ether (2.5 mL) was added, the solution was kept at 30°C. The brown crystals of $\mathbf{IV_{CrMn4Lu2}}$ suitable for X-ray crystallographic analysis were obtained after 1 day (81.2 mg, 51% yield based on $\mathbf{II_{CrMn4}}$). IR (KBr pellet): 2961, 2932, 2873, 1617, 1521, 1465, 1408, 1384, 1266, 1153, 1110, 1061, 1015, 960, 939, 889, 792, 757, 645, 536, 458, 414, 391, 369, 336, 316, 303, 291, 282, 255 cm^{-1}; positive ion MS (CSI, acetonitrile): *m/z* 3843 (calcd. 3842.8) $[TBA_9Si_2W_{18}O_{70}CrMn_4Lu_2(acac)_4]^{2+}$, 7443 (calcd. 7443.1) $[TBA_8Si_2W_{18}O_{70}CrMn_4Lu_2(acac)_4]^+$; elemental analysis

calcd (%) for $TBA_7[(SiW_9O_{34})_2CrMn_4O_2\{Lu(acac_2)\}_2]\cdot 3C_2H_4Cl_2\cdot H_2O$ ($C_{138}H_{294}Cl_6CrLu_2Mn_4N_7O_{79}Si_2W_{18}$), C 22.05, H 3.94, N 1.30, Si 0.75, Cr 0.69, Mn 2.92, Lu 4.66, W 44.03; found, C 21.92, H 3.94, N 1.31, Si 0.73, Cr 0.69, Mn 2.66, Lu 4.40, W 44.75.

Synthesis and Characterization of $TBA_5[(A\text{-}\alpha\text{-}SiW_9O_{34})_2CrMn_4O_2\{Lu(C_5H_7O_2)_2\}_2Ag_2]\cdot 4H_2O\cdot CH_3CN$ ($V_{CrMn4Lu2Ag2}$): To an acetonitrile solution (2 mL) of $IV_{CrMn4Lu2}$ (80.9 mg, 10.8 μmol), AgOTf (5.5 mg, 21.6 μmol) was added, and the resulting solution was stirred for 4 h at room temperature (ca. 20°C). Then, diethyl ether (6.4 mL) was added to the solution and the solution was filtered off. The brown crystals of $V_{CrMn4Lu2Ag2}$ suitable for X-ray crystallographic analysis were obtained after 1 day (45.5 mg, 60% yield based on $IV_{CrMn4Lu2}$). IR (KBr pellet): 2961, 2931, 2874, 1617, 1523, 1479, 1458, 1403, 1384, 1269, 1153, 1105, 1065, 1017, 963, 941, 889, 791, 756, 645, 538, 388, 366, 336, 322, 310, 298, 283, 278, 267, 254 cm^{-1}; positive ion MS (CSI, acetonitrile): *m/z* 3708 (calcd. 3708.2) $[TBA_7Si_2W_{18}O_{70}CrMn_4Lu_2(acac)_4Ag_2]^{2+}$, 7174 (calcd. 7173.9) $[TBA_6Si_2W_{18}O_{70}CrMn_4Lu_2(acac)_4Ag_2]^{+}$; elemental analysis calcd (%) for $TBA_5[(SiW_9O_{34})_2CrMn_4O_2\{Lu(acac)_2\}_2Ag_2]\cdot 4H_2O\cdot CH_3CN$ ($C_{120}H_{219}Ag_2CrLu_2Mn_4N_6O_{82}Si_2W_{18}$), C 17.39, H 3.13, N 1.19, Si 0.80, W 46.97, Cr 0.74, Mn 3.12, Lu 4.97, Ag 3.06; found, C 17.40, H 3.14, N 1.11, Si 0.79, W 46.80, Cr 0.74, Mn 2.85, Lu 4.61, Ag 3.06.

Table S1. Cr-containing POMs.

Entry	Formula	Reference
1	$[SiW_9O_{37}Cr_3(OH)_3]^{7-}$	S10a, S10b
2	$[\{A\text{-}\alpha\text{-}SiW_9O_{34}Cr_3(OH)_3\}_2(OH)_3]^{11-}$	S10c
3	$[(HXW_7O_{28})_2Cr]^{13-}$ (X = P, As)	S10d
4	$[\gamma\text{-}SiW_{10}O_{32}(OH)_2Cr_2(CH_3CO_2)_2(OH_2)_2]^{5-}$	S10e
5	$[(\gamma\text{-}SiW_{10}O_{36})_2\{Cr(OH)(H_2O)\}_3]^{10-}$	S10f
6	$[(\gamma\text{-}SiW_{10}O_{36})_2\{Cr(OH)(H_2O)\}_3\{La(H_2O)_7\}_2]^{4-}$	S10f
7	$[(B\text{-}\beta\text{-}XW_8O_{31})_2Cr_2]^{14-}$ (X = Si, Ge)	S10g
8	$[(AsMo_7O_{27})_2Cr_2]^{12-}$	S10h
9	$[(AsMo_7O_{27})_2CrFe]^{12-}$	S10i
10	$[\alpha\text{-}PW_{11}O_{39}Cr(OH_2)]^{4-}$	S10j
11	$[\alpha\text{-}P_2W_{17}O_{61}Cr(OH_2)]^{7-}$	S10j

Table S2. Crystallographic data of $\mathbf{I_{Cr}}$, $\mathbf{II_{CrMn4}}$, $\mathbf{III_{CrMn4Ag2}}$, $\mathbf{IV_{CrMn4Lu2}}$, and $\mathbf{V_{CrMn4Lu2Ag2}}$.

	$\mathbf{I_{Cr}}$	$\mathbf{II_{CrMn4}}$	$\mathbf{III_{CrMn4Ag2}}$	$\mathbf{IV_{CrMn4Lu2}}$	$\mathbf{V_{CrMn4Lu2Ag2}}$
molecular formula	$C_{124}Cl_{12}CrN_7O_{70}Si_2W_{18}$	$C_{120}Cl_8CrMn_4N_7O_{70}Si_2W_{18}$	$C_{84}Ag_2CrMn_4N_7O_{70}Si_2W_{18}$	$C_{132}Cl_8CrLu_2Mn_4N_7O_{78}Si_2W_{18}$	$C_{116}CrAg_2Lu_2Mn_4N_{13}O_{78}Si_2W_{18}$
Fw (g mol^{-1})	6550.19	6580.11	6079.89	7202.17	7026.22
crystal system	triclinic	triclinic	triclinic	triclinic	triclinic
space group	*P*-1 (No. 2)	*P*-1 (No. 2)	*P*-1 (No. 2)	*P*-1 (No. 2)	*P*-1 (No. 2)
a (Å)	14.6870(3)	14.32460(10)	14.5907(2)	19.3682(2)	17.4607(3)
b (Å)	18.7174(5)	20.0905(2)	14.8029(2)	22.8418(3)	18.5296(6)
c (Å)	19.0467(4)	34.1760(4)	19.3294(3)	26.9735(4)	19.3013(3)
α (deg)	106.2000(10)	102.4516(6)	68.6210(10)	87.3100(10)	61.2950(10)
β (deg)	92.3250(10)	96.5392(6)	80.4000(10)	78.6320(10)	63.2520(10)
γ (deg)	97.7920(10)	93.5466(4)	66.5450(10)	85.3220(10)	82.4150(10)
volume (Å^3)	4964.7(2)	9503.70(17)	3565.21(9)	11654.3(3)	4862.9(2)
Z	1	2	1	2	1
temp (K)	123(2)	123(2)	123(2)	123(2)	123(2)
ρ_{calcd} (g cm^{-3})	2.191	2.299	2.832	2.052	2.399
GOF	1.066	1.091	1.137	1.086	1.033
R_1[a] [$I > 2\sigma(I)$]	0.0899	0.0611	0.0590	0.0787	0.0506
wR_2[a]	0.2950	0.1965	0.1977	0.2579	0.1420

[a] $R_1 = \Sigma||F_o|-|F_c||/\Sigma|F_o|$, $wR_2 = \{\Sigma[w(F_o^2-F_c^2)]/\Sigma[w(F_o^2)^2]\}^{1/2}$.

Table S3. BVS values of oxygen and metal atoms of $\mathbf{I_{Cr}}$.

O1	1.581	O24	2.021
O2	1.629	O25	2.028
O3	0.637	O26	1.854
O4	1.039	O27	1.935
O5	0.635	O28	1.963
O6	0.806	O29	1.882
O7	1.822	O30	1.905
O8	1.783	O31	1.860
O9	1.822	O32	1.671
O10	1.740	O33	1.627
O11	1.667	O34	1.680
O12	1.698	Si1	3.911
O13	1.892	Cr1	2.998
O14	2.106	W1	6.205
O15	1.921	W2	5.916
O16	2.103	W3	6.143
O17	2.041	W4	5.807
O18	2.146	W5	5.854
O19	1.899	W6	5.955
O20	1.883	W7	5.965
O21	1.883	W8	5.906
O22	1.912	W9	5.911
O23	2.001		

Table S4. Intramolecular exchange interactions and selected average bond angles in $\mathbf{II}_{\mathbf{CrMn4}}$, $\mathbf{III}_{\mathbf{CrMn4Ag2}}$, $\mathbf{IV}_{\mathbf{CrMn4Lu2}}$, and $\mathbf{V}_{\mathbf{CrMn4Lu2Ag2}}$.

	J_1 (cm^{-1})	J_2 (cm^{-1})	∠Cr–O–Mn (º)	∠Mn–O–Mn (º)
$\mathbf{II}_{\mathbf{CrMn4}}$	–3.48	–2.94	130.15	128.22
$\mathbf{III}_{\mathbf{CrMn4Ag2}}$	–2.14	–3.29	129.09	128.48
$\mathbf{IV}_{\mathbf{CrMn4Lu2}}$	–0.07	–8.46	127.88	129.35
$\mathbf{V}_{\mathbf{CrMn4Lu2Ag2}}$	–0.48	–5.58	128.19	127.42

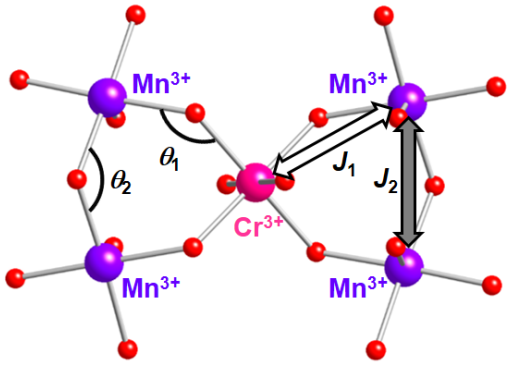

Table S5. BVS values of oxygen and metal atoms of $\mathbf{II}_{\mathbf{CrMn4}}$.

O1	2.066	O33	1.726	O65	1.769
O2	2.051	O34	1.887	O66	1.900
O3	1.865	O35	1.832	O67	1.764
O4	1.810	O36	1.877	O68	1.936
O5	1.861	O37	2.038	O1H	1.143
O6	1.890	O38	2.062	O2H	1.149
O7	1.703	O39	1.861	Si1	3.975
O8	1.712	O40	1.827	Si2	3.957
O9	1.717	O41	1.708	Cr1	2.987
O10	1.793	O42	1.928	Mn1	2.922
O11	1.812	O43	1.726	Mn2	2.974
O12	1.712	O44	2.038	Mn3	2.940
O13	1.976	O45	1.736	Mn4	2.940
O14	2.028	O46	1.997	W1	6.052
O15	1.913	O47	1.740	W2	6.136
O16	1.973	O48	2.024	W3	6.002
O17	1.989	O49	1.717	W4	6.103
O18	2.058	O50	1.942	W5	6.079
O19	1.932	O51	1.745	W6	6.057
O20	2.009	O52	1.971	W7	6.103
O21	2.016	O53	2.007	W8	5.993
O22	2.036	O54	1.936	W9	6.034
O23	1.958	O55	2.001	W10	6.128
O24	2.019	O56	2.045	W11	6.067
O25	2.019	O57	1.995	W12	6.070
O26	1.979	O58	1.991	W13	6.034
O27	2.026	O59	2.029	W14	6.014
O28	1.952	O60	1.972	W15	5.997
O29	1.662	O61	2.021	W16	6.055
O30	1.920	O62	1.953	W17	6.121
O31	1.703	O63	1.703	W18	6.037
O32	1.976	O64	1.942		

Table S6. BVS values of oxygen and metal atoms of $\mathbf{III}_{\mathbf{CrMn4Ag2}}$.

O1	2.038	O19	1.941	Cr1	2.958
O2	2.123	O20	2.000	Mn1	3.013
O3	1.926	O21	1.989	Mn2	2.979
O4	1.888	O22	1.960	Ag1	0.928
O5	1.817	O23	2.060	W1	6.157
O6	1.868	O24	2.043	W2	6.069
O7	1.740	O25	2.053	W3	6.109
O8	1.694	O26	2.043	W4	6.084
O9	1.754	O27	2.054	W5	6.018
O10	1.717	O28	2.043	W6	5.965
O11	1.722	O29	1.950	W7	6.096
O12	1.736	O30	1.975	W8	6.110
O13	1.975	O31	1.962	W9	6.101
O14	2.108	O32	1.764		
O15	2.021	O33	1.764		
O16	2.041	O34	1.798		
O17	1.968	O1H	1.162		
O18	2.106	Si1	3.954		

Table S7. BVS values of oxygen and metal atoms of $\mathbf{IV}_{\mathbf{CrMn4Lu2}}$.

O1	2.097	O37	1.837	O73	1.832
O2	2.081	O38	1.815	O74	1.940
O3	1.915	O39	1.808	O75	1.738
O4	1.902	O40	2.086	O76	1.895
O5	1.970	O41	2.042	O77	2.018
O6	1.921	O42	1.921	O78	1.912
O7	1.667	O43	1.903	Si1	4.002
O8	1.722	O44	2.013	Si2	3.991
O9	1.717	O45	1.907	Cr1	2.961
O10	1.862	O46	1.778	Cr2	2.991
O11	1.726	O47	1.712	Mn11	2.874
O12	1.698	O48	1.708	Mn12	2.923
O13	2.050	O49	1.764	Mn21	2.927
O14	2.070	O50	1.793	Mn22	2.832
O15	1.929	O51	1.708	Lu1	3.236
O16	2.014	O52	1.982	Lu2	3.251
O17	2.079	O53	2.083	W1	6.035
O18	2.113	O54	1.989	W2	6.164
O19	1.941	O55	1.997	W3	6.140
O20	2.013	O56	2.005	W4	6.136
O21	1.996	O57	2.070	W5	6.217
O22	1.996	O58	1.904	W6	6.166
O23	2.066	O59	2.012	W7	6.096
O24	2.092	O60	2.026	W8	6.037
O25	1.972	O61	1.991	W9	6.013
O26	2.083	O62	2.078	W10	6.232
O27	2.061	O63	2.056	W11	6.043
O28	1.972	O64	1.942	W12	6.141
O29	1.906	O65	2.040	W13	6.029
O30	1.976	O66	2.086	W14	6.234
O31	1.952	O67	1.985	W15	6.100
O32	1.708	O68	1.910	W16	6.195
O33	1.662	O69	1.973	W17	6.000
O34	1.722	O70	1.962	W18	6.165
O35	1.945	O71	1.764		
O36	1.775	O72	1.769		

Table S8. BVS values of oxygen and metal atoms of $V_{CrMn4Lu2Ag2}$.

O1	2.078	O19	1.942	O37	1.885
O2	2.073	O20	2.023	O38	1.906
O3	1.898	O21	2.031	O39	1.848
O4	1.977	O22	1.998	Si1	4.022
O5	1.982	O23	2.077	Cr1	2.964
O6	1.870	O24	2.093	Mn1	2.986
O7	1.712	O25	1.972	Mn2	2.982
O8	1.740	O26	2.069	Ag1	0.994
O9	1.712	O27	2.084	Lu1	3.320
O10	1.793	O28	2.002	W1	6.103
O11	1.774	O29	1.939	W2	6.107
O12	1.827	O30	2.012	W3	6.080
O13	2.125	O31	1.990	W4	6.132
O14	2.051	O32	1.754	W5	6.098
O15	2.041	O33	1.857	W6	6.128
O16	2.029	O34	1.731	W7	6.176
O17	1.953	O35	1.959	W8	6.242
O18	2.074	O36	1.982	W9	6.141

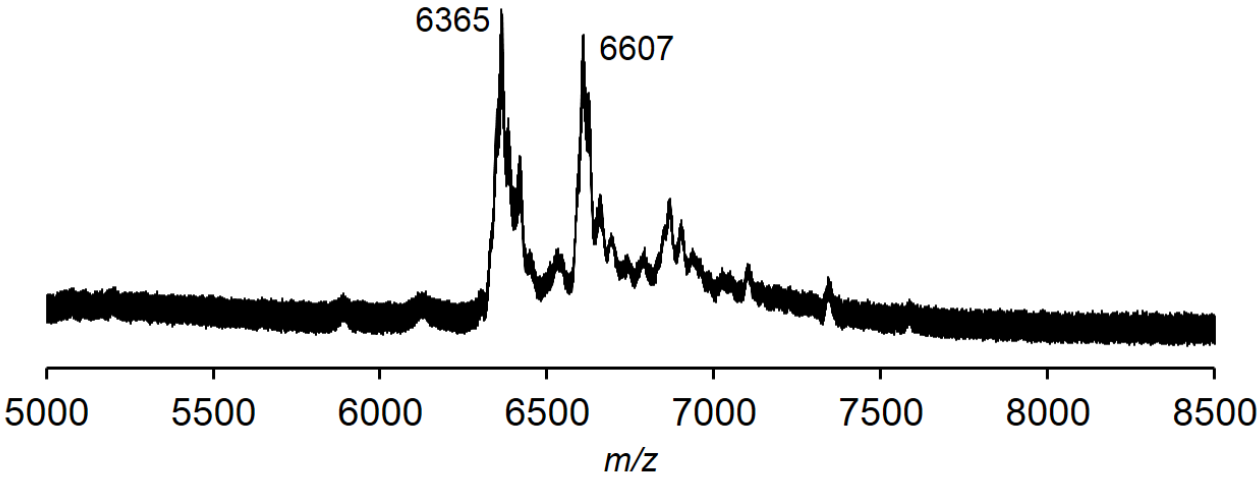

Fig. S1 Positive-ion CSI mass spectrum of the synthetic solution of $\mathbf{I_{Cr}}$ in acetone. The sets of signals centered at *m/z* 6365 and 6607 were assignable to $[TBA_8Si_2W^{6+}{}_{18}O_{63}Cr^{3+}]^+$ and $[TBA_9Si_2W^{6+}{}_{17}W^{5+}O_{63}Cr^{3+}]^+$.

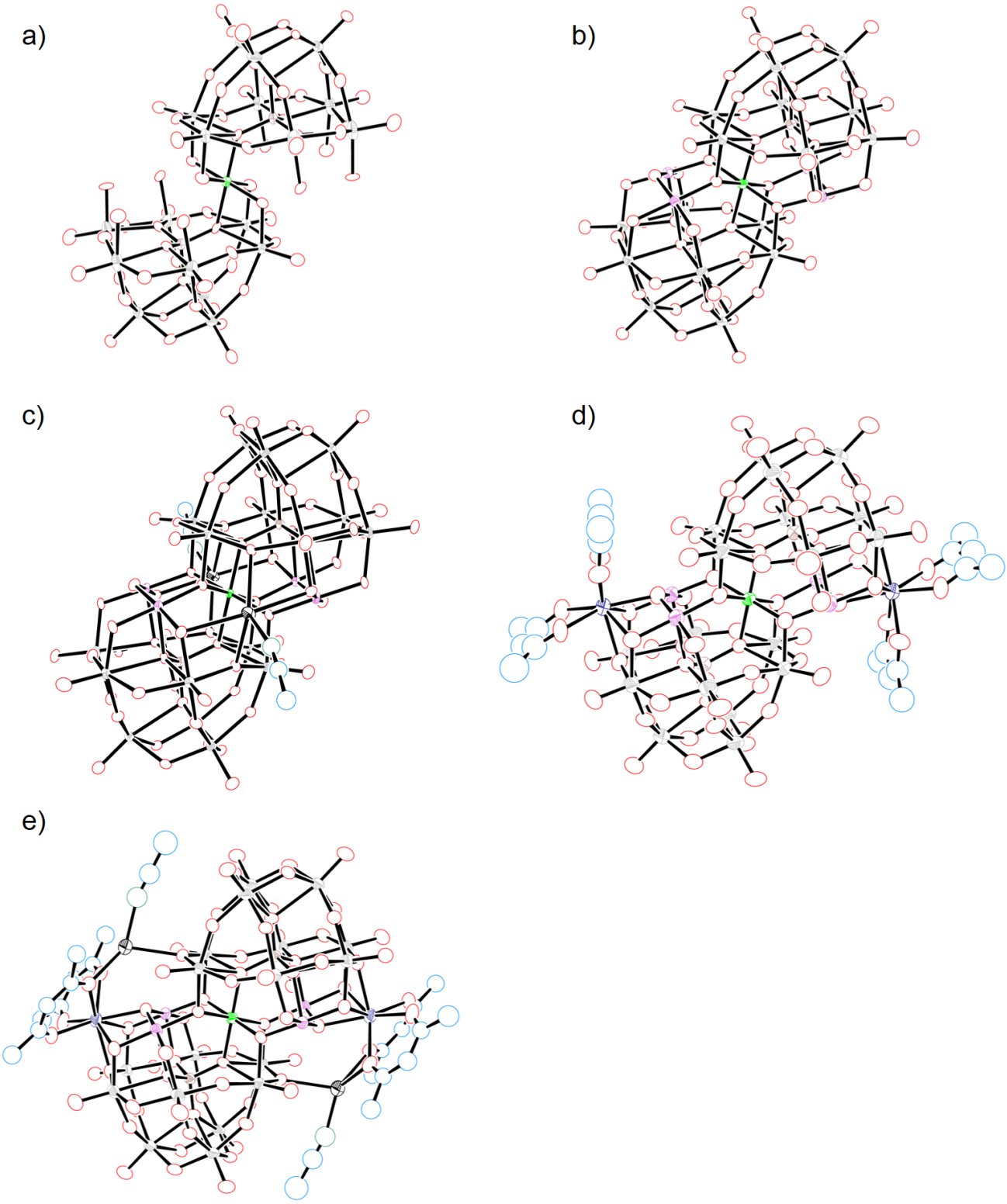

Fig. S2 ORTEP representations of the anion parts of a) $\mathbf{I}_{\mathbf{Cr}}$, b) $\mathbf{II}_{\mathbf{CrMn4}}$, c) $\mathbf{III}_{\mathbf{CrMn4Ag2}}$, d) $\mathbf{IV}_{\mathbf{CrMn4Lu2}}$, and e) $\mathbf{V}_{\mathbf{CrMn4Lu2Ag2}}$ with thermal ellipsoids drawn at the 50% probability level.

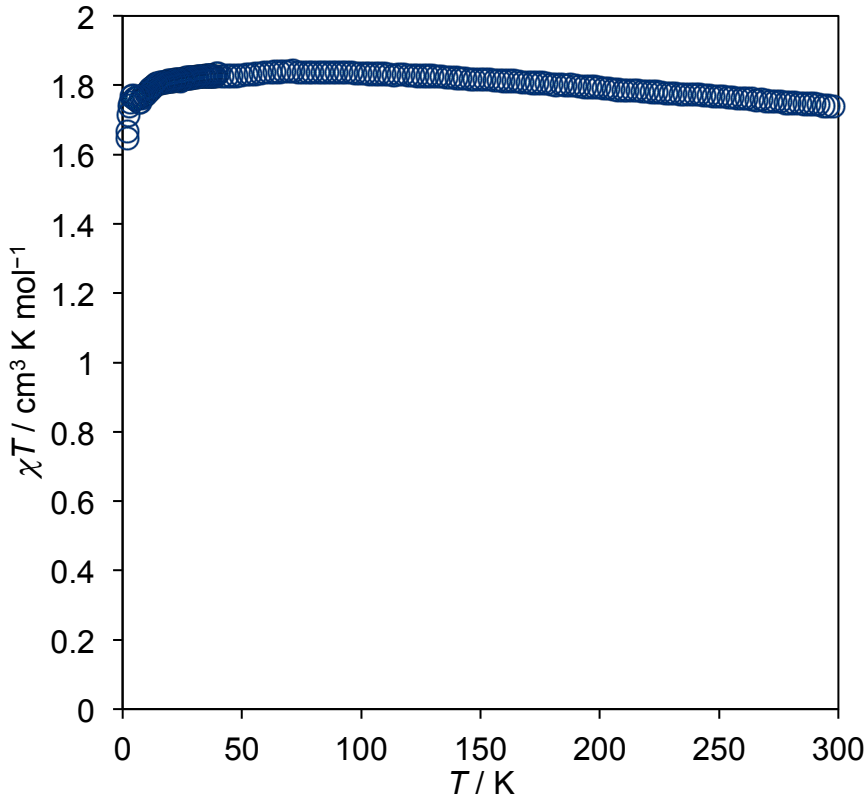

Fig. S3 Temperature dependence of χT for $\mathbf{I_{Cr}}$ under 0.1 T.

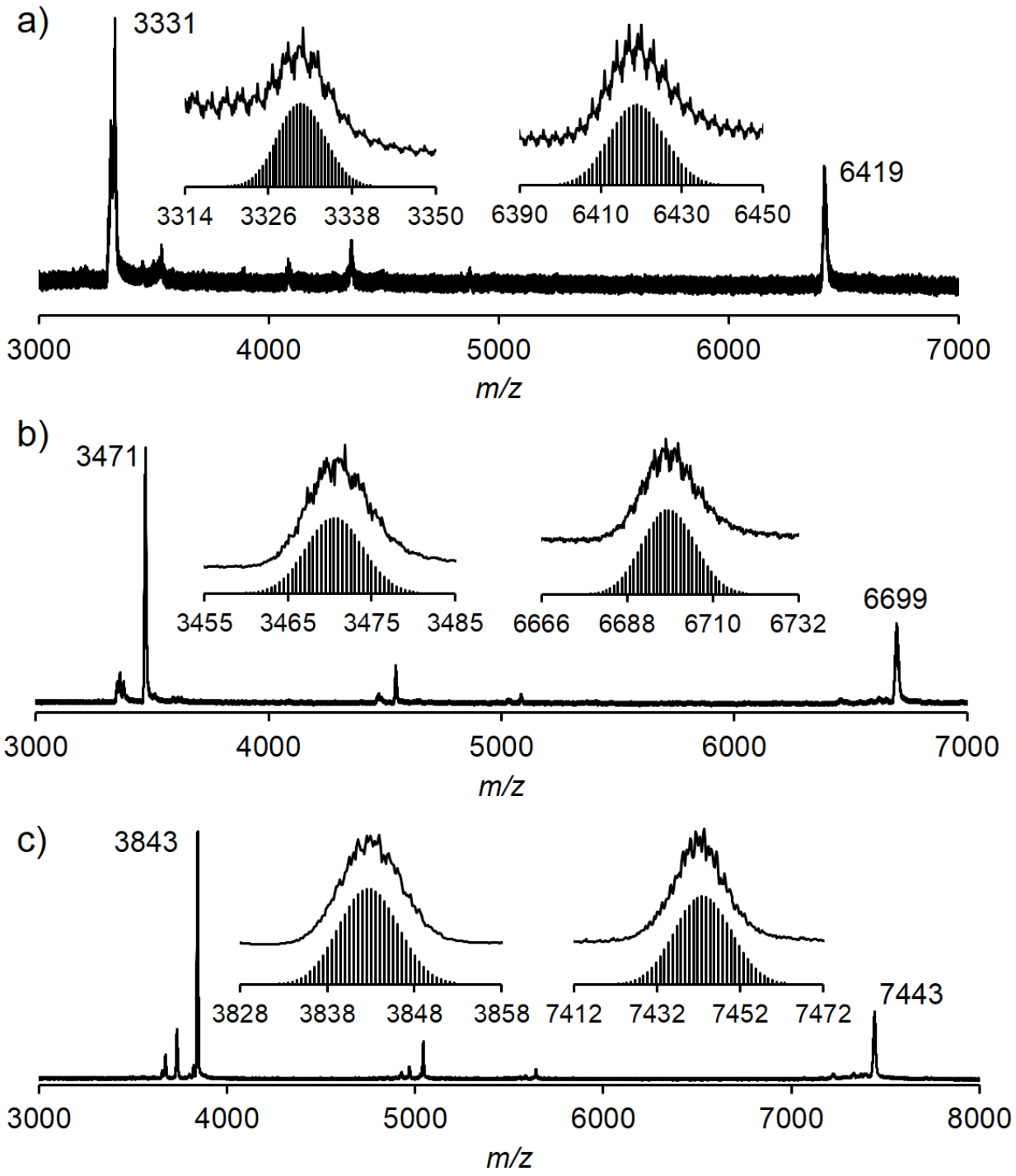

Fig. S4 Positive-ion CSI mass spectra of a) $\mathbf{I}_{\mathbf{Cr}}$, b) $\mathbf{II}_{\mathbf{CrMn4}}$ in 1,2-dichloroethane, and c) $\mathbf{IV}_{\mathbf{CrMn4Lu2}}$ in acetonitrile. Insets: a) spectra in the range of *m/z* 3314–3350 and 6390–6450, and simulated patterns for $[TBA_9H_6Si_2W_{18}O_{66}Cr]^{2+}$ (*m/z* 3330.8) and $[TBA_8H_6Si_2W_{18}O_{66}Cr]^{+}$ (*m/z* 6419.0); b) spectra in the range of *m/z* 3455–3485 and 6666–6732, and simulated patterns for $[TBA_9H_2Si_2W_{18}O_{70}CrMn_4]^{2+}$ (*m/z* 3470.6) and $[TBA_8H_2Si_2W_{18}O_{70}CrMn_4]^{+}$ (*m/z* 6698.7); c) spectra in the range of *m/z* 3828–3858 and 7412–7472, and simulated patterns for $[TBA_9Si_2W_{18}O_{70}CrMn_4Lu_2(acac)_4]^{2+}$ (*m/z* 3842.8) and $[TBA_8Si_2W_{18}O_{70}CrMn_4Lu_2(acac)_4]^{+}$ (*m/z* 7443.1).

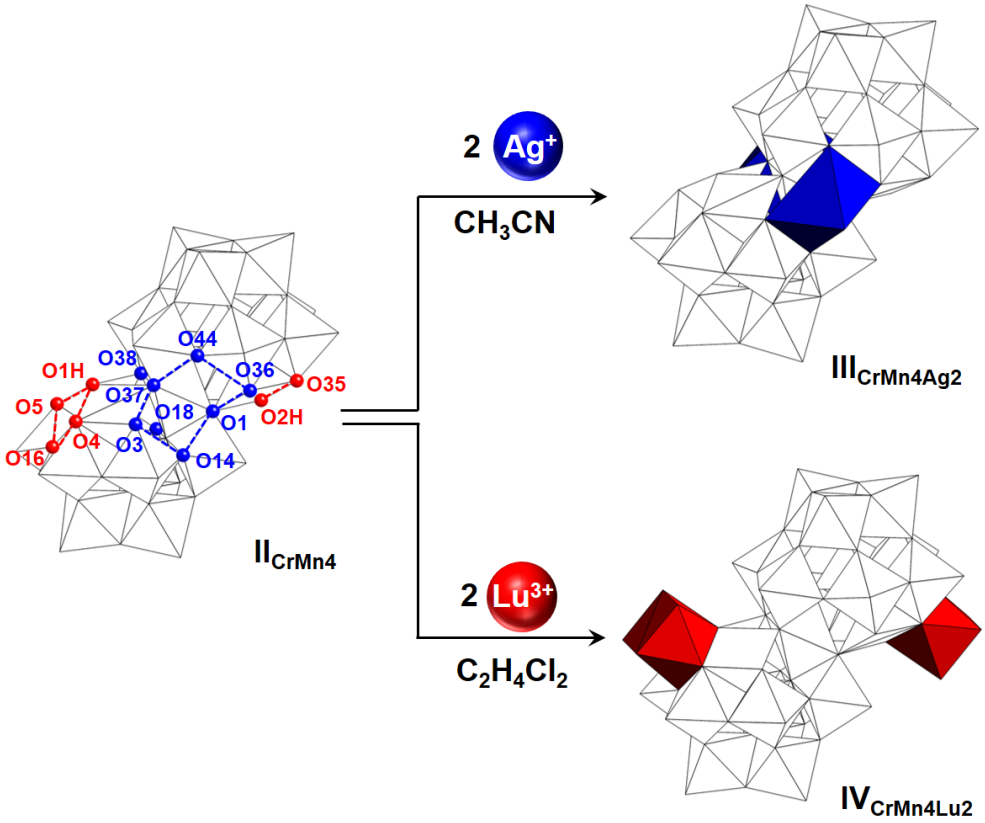

Fig. S5 Two types of pseudo vacant sites in $\mathbf{II}_{\mathbf{CrMn4}}$ for the introduction of Ag^{+} and Lu^{3+}. The oxygen atoms at the pseudo vacant sites were represented by spheres (blue, long side; red, short side).

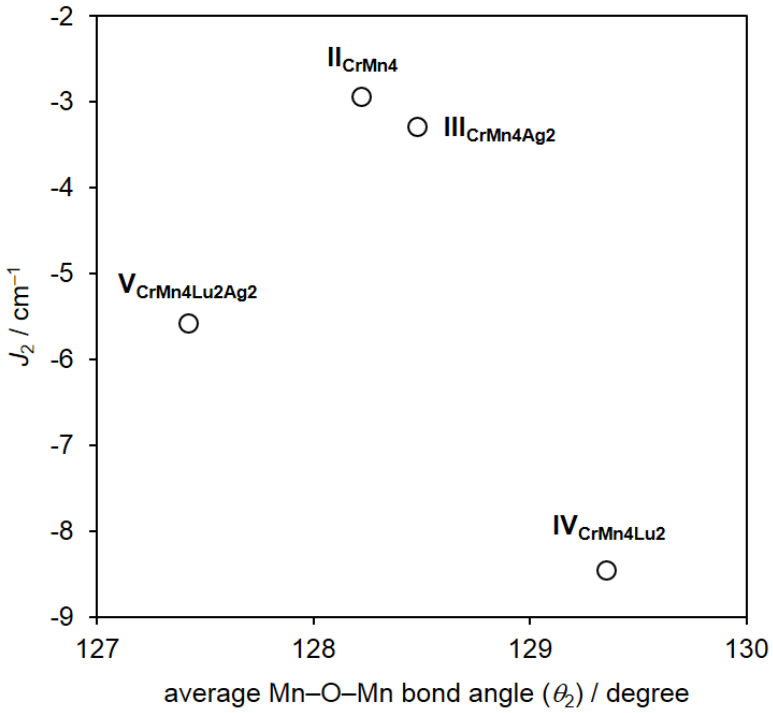

Fig. S6 Magnetostructural correlation between the average Mn–O–Mn bond angles (θ_2) and values of J_2.

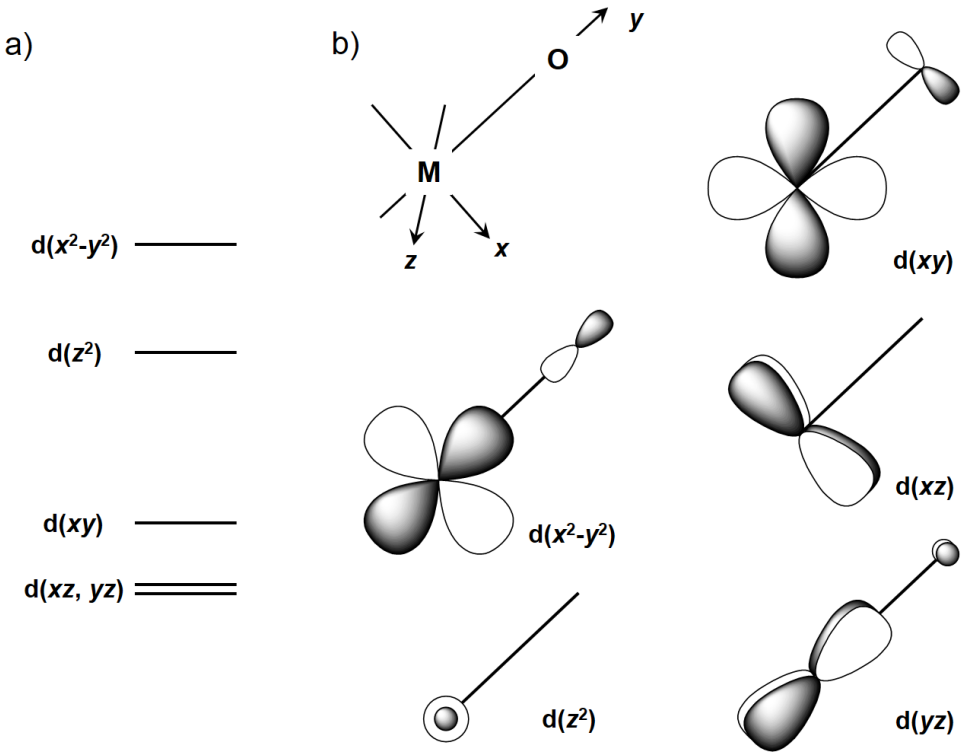

Fig. S7. a) Expected d orbital splitting of Cr^{3+} (d^3) and Mn^{3+} (d^4, high spin) in the {$CrMn_4$} unit and b) their local orbitals (M = Cr^{3+}, Mn^{3+}) by matching the Jahn−Teller and *z* axes.

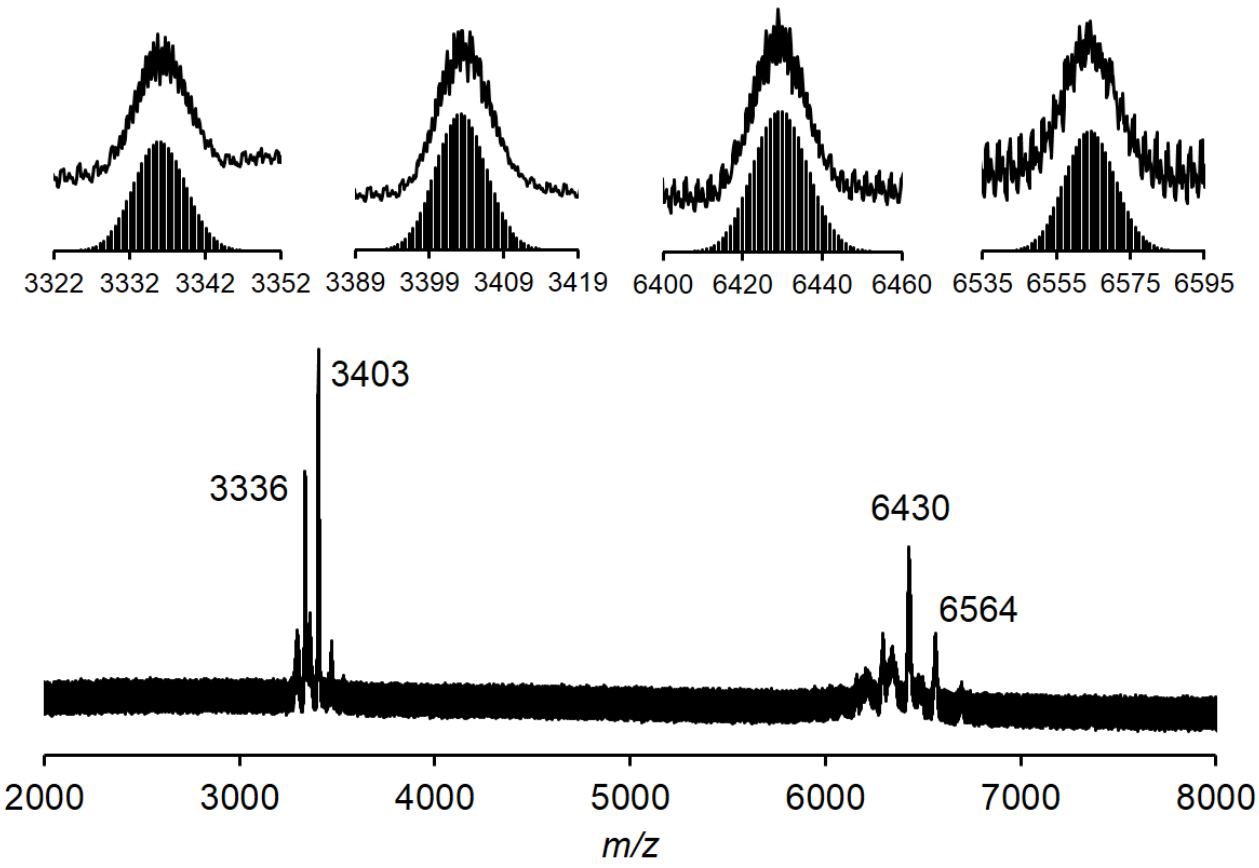

Fig. S8 Positive-ion CSI mass spectra of $\mathbf{III}_{\mathbf{CrMn4Ag2}}$ in acetonitrile. Insets: spectra in the range of *m/z* 3322–3352, 3389–3419, 6400–6460, and 6535–6595, and simulated patterns for $[TBA_7H_2Si_2W_{18}O_{70}CrMn_4Ag_2]^{2+}$ (*m/z* 3336.0), $[TBA_8H_2Si_2W_{18}O_{70}CrMn_4Ag]^{2+}$ (*m/z* 3403.3), $[TBA_6H_2Si_2W_{18}O_{70}CrMn_4Ag_2]^{+}$ (*m/z* 6429.5) and $[TBA_7H_2Si_2W_{18}O_{70}CrMn_4Ag]^{+}$ (*m/z* 6564.1).

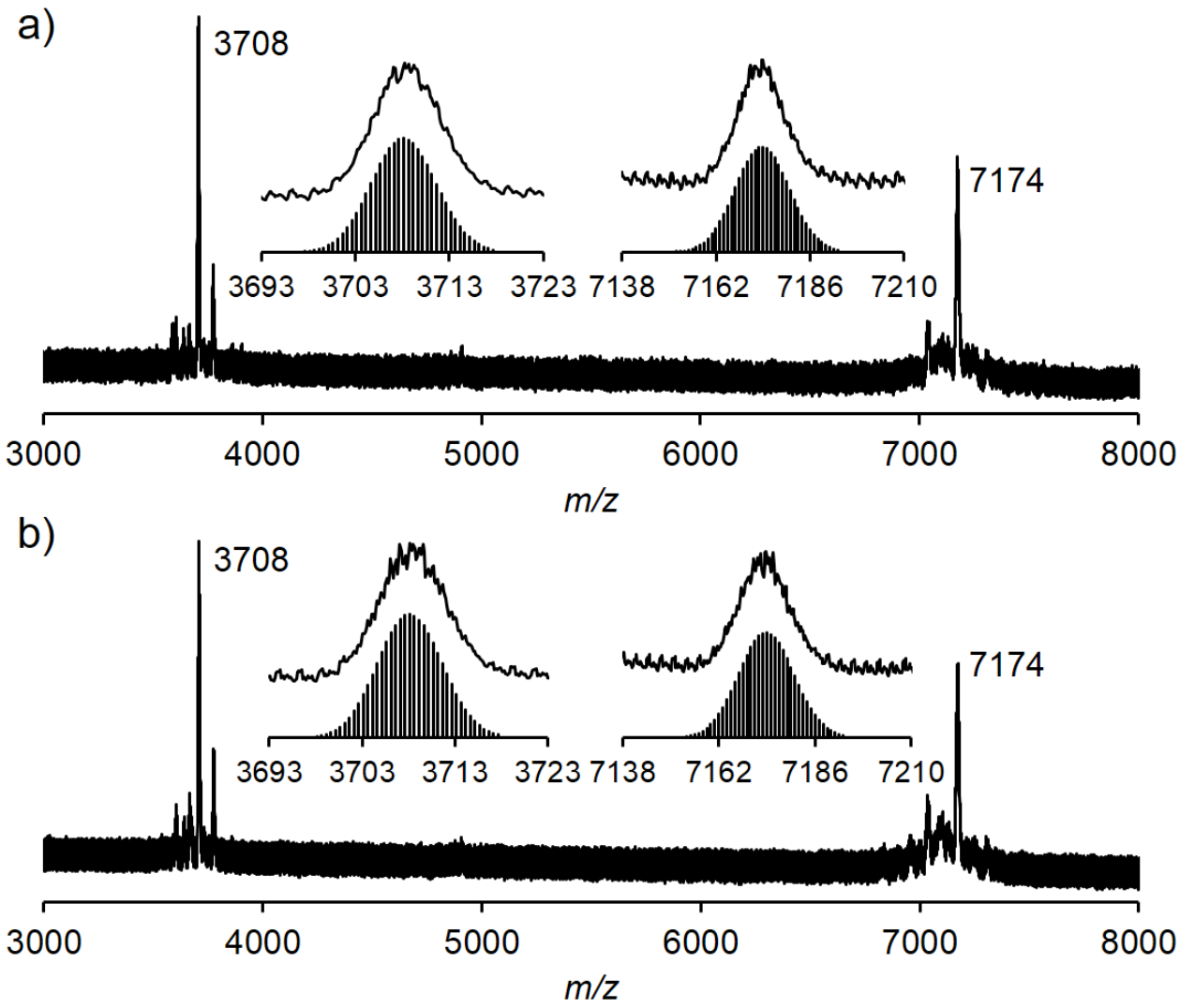

Fig. S9 Positive-ion CSI mass spectra in acetonitrile. a) $\mathbf{V_{CrMn4Lu2Ag2}}$ synthesized by the reaction of $\mathbf{IV_{CrMn4Lu2}}$ with Ag^{+} and b) $\mathbf{V_{CrMn4Lu2Ag2}}$ synthesized by the reaction of $\mathbf{III_{CrMn4Ag2}}$ with Lu^{3+}. Insets: spectra in the range of *m/z* 3693–3723 and 7138–7210, and simulated patterns for $[TBA_7Si_2W_{18}O_{70}CrMn_4Lu_2(acac)_4Ag_2]^{2+}$ (*m/z* 3708.2) and $[TBA_6Si_2W_{18}O_{70}CrMn_4Lu_2(acac)_4Ag_2]^{+}$ (*m/z* 7173.9).

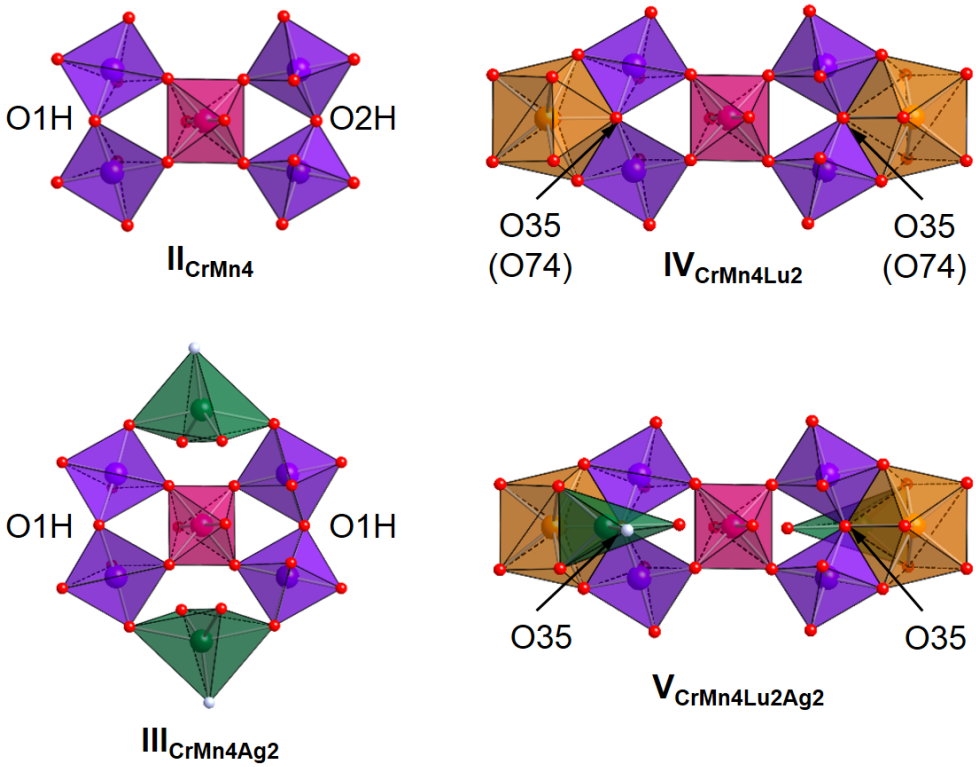

Fig. S10 Multinuclear heterometallic oxo clusters in $\mathbf{II}_{\mathbf{CrMn4}}$, $\mathbf{III}_{\mathbf{CrMn4Ag2}}$, $\mathbf{IV}_{\mathbf{CrMn4Lu2}}$, and $\mathbf{V}_{\mathbf{CrMn4L2Ag2}}$.

References

S1 T. Minato, K. Suzuki, K. Kamata and N. Mizuno, *Chem. –Eur. J.*, 2014, **20**, 5946.

S2 (*a*) *CrystalClear* 1.3.6, Rigaku and Rigaku/MSC, The Woodlands, TX; (*b*) J. W. Pflugrath, *Acta Crystallogr.*, 1999, **D55**, 1718.

S3 Z. Otwinowski and W. Minor, Processing of X-ray Diffraction Data Collected in Oscillation Mode in *Methods in Enzymology*, C. W. Carter, Jr., R. M. Sweet, Eds., Macromolecular Crystallography, Part A, Academic press, New York, 1997, **276**, 307.

S4 *CrystalStructure* 3.8, Rigaku and Rigaku/MSC, TheWoodlands, TX.

S5 L. J. Farrugia, *J. Appl. Crystallogr.*, 1999, **32**, 837.

S6 (*a*) G. M. Sheldrick, SHELX97, *Programs for Crystal Structure Analysis*, Release 97-2, University of Göttingen, Göttingen, Germany, 1997; (*b*) G. M. Sheldrick, SHELX-2014, *Programs for Crystal Structure Analysis*, University of Göttingen, Göttingen, Germany, 2014.

S7 (*a*) I. D. Brown and D. Altermatt, *Acta Crystallogr.*, 1985, **B41**, 244; (*b*) N. E. Brese and M. O'Keeffe, *Acta Crystallogr.*, 1991, **B47**, 192.

S8 N. F. Chilton, R. P. Anderson, L. D. Turner, A. Soncini and K. S. Murray, *J. Comput. Chem.*, 2013, **34**, 1164.

S9 H. S. Booth, *Inorg. Synth.*, 1939, **1**, 122.

S10 (*a*) J. Peng, L.-Y. Qu and Y.-G. Chen, *Inorg. Chem. Acta.*, 1991, **183**, 157; (*b*) K. Wassermann, H.-J. Lunk, R. Palm and J. Fuchs, *Acta Cryst.*, 1994, **C50**, 348; (*c*) K. Wassermann, H.-J. Lunk, R. Palm, J. Fuchs, N. Steinfeldt, R. Stösser and M. T. Pope, *Inorg. Chem.*, 1996, **35**, 3273; (*d*) W. Liu, J. H. Christian, R. Al-Oweini, B. S. Bassil, J. van Tol, M. Atanasov, F. Neese, N. S. Dalal and U. Kortz, *Inorg. Chem.*, 2014, **53**, 9274; (*e*) K. Wassermann, R. Palm, H.-J. Lunk, J. Fuchs, N. Steinfeldt and R. Stösser, *Inorg. Chem.*, 1995, **34**, 5029; (*f*) J.-D. Compain, P. Mialane, A. Dolbecq, I. M. Mbomekallé, J. Marrot, F. Sécheresse, C. Duboc and E. Riviére, *Inorg. Chem.*, 2010, **49**, 2851; (*g*) W. Liu, R. Al-Oweini, K. Meadows, B. S. Bassil, Z. Lin, J. H. Christian, N. S. Dalal, A. M. Bossoh, I. M. Mbomekallé, P. de Oliveira, J. Iqbal and U. Kortz, *Inorg. Chem.*, 2016, **55**, 10936; (*h*) L. Li, Q. Shen, G. Xue, H. Xu, H. Hu, F. Feng and J. Wang, *Dalton Trans.*, 2008, 5698; (*i*) H. Xu, L. Li, B. Liu, G.

Xue, H. Hu, F. Fu and J. Wang, *Inorg. Chem.*, 2009, **48**, 10275; (*j*) C. Rong and F. C. Anson, *Inorg. Chem.*, 1994, **33**, 1064.